

Experimental Observation of Partial Parity-Time Symmetry and Its Phase Transition with a Laser-Driven Cesium Atomic Gas

Yongmei Xue^{1,*}, Chao Hang^{2,3,4,*}, Yunhui He¹, Zhengyang Bai², Yuechun Jiao^{1,4}, Guoxiang Huang^{2,3,4,†}, Jianming Zhao^{1,4,‡} and Suotang Jia^{1,4}

¹State Key Laboratory of Quantum Optics and Quantum Optics Devices, Institute of Laser Spectroscopy, Shanxi University, Taiyuan 030006, China

²State Key Laboratory of Precision Spectroscopy, East China Normal University, Shanghai 200062, China

³NYU-ECNU Joint Institute of Physics, New York University Shanghai, Shanghai 200062, China and

⁴Collaborative Innovation Center of Extreme Optics, Shanxi University, Taiyuan, Shanxi 030006, China

(Dated: September 21, 2021)

Realization and manipulation of parity-time (\mathcal{PT}) symmetry in multidimensional systems are highly desirable for exploring nontrivial physics and uncovering exotic phenomena in non-Hermitian systems. Here, we report the first experimental observation of partial \mathcal{PT} ($\text{p}\mathcal{PT}$) symmetry in a cesium atomic gas coupled with laser fields, where a two-dimensional $\text{p}\mathcal{PT}$ -symmetric optical potential for probe laser beam is created. A transition of the $\text{p}\mathcal{PT}$ symmetry from an unbroken phase to a broken one is observed through changing the beam-waist ratio of the control and probe laser beams, and the domains of unbroken, broken, and non- $\text{p}\mathcal{PT}$ phases are also discriminated unambiguously. Moreover, we develop a technique to precisely determine the location of the exceptional point of the $\text{p}\mathcal{PT}$ symmetry breaking by measuring the asymmetry degree of the probe-beam intensity distribution. The findings reported here pave the way for controlling multidimensional laser beams in non-Hermitian systems via laser-induced atomic coherence, and have potential applications for designing new types of light amplifiers and attenuators.

Introduction.— Although non-Hermitian Hamiltonians generally have complex eigenvalues, a wide class of non-Hermitian Hamiltonians with parity-time (\mathcal{PT}) symmetry was found to exhibit all-real spectra [1–5]. The exploration of \mathcal{PT} -symmetry has provided an excellent platform for uncovering the exotic behaviors in systems with open environments and spawned intriguing prospects of non-Hermitian physics [6]. The study of \mathcal{PT} -symmetric Hamiltonians was soon introduced into optics [7–10] based on a close analogy between the Schrödinger equation in quantum mechanics and the Maxwell equation under paraxial approximation in electrodynamics. An optical \mathcal{PT} symmetry can be created when the potential $V(\mathbf{r})$ controlling light propagation is made to be invariant under complex conjugation and simultaneous reflection in all spatial directions, i.e. $V^*(\mathbf{r}) = V(-\mathbf{r})$. In recent years, there have been intensive studies on the realization of optical \mathcal{PT} symmetry in various physical settings, including waveguide and fiber arrays [11–13], photonic circuits and lattices [14, 15], microtoroid resonators [16–18], trapped ions [19], etc. Compared to other materials, atomic media are desirable for realizing non-Hermitian Hamiltonians by synthesizing desired refractive index profiles due to their nice coherence property and the superiority for available active manipulations on light absorption, gain, dispersion, and nonlinearity, and so on [20–27].

Note that to have an all-real spectrum for a non-Hermitian Hamiltonian, the condition of \mathcal{PT} symmetry is neither sufficient nor necessary. When non-Hermiticity increases, the spectrum of a \mathcal{PT} -symmetric Hamiltonian

will become complex, indicating that a phase transition occurs from unbroken \mathcal{PT} phase to broken \mathcal{PT} phase. The transition point between the unbroken and broken phases is called exceptional point (EP), at which both eigenstates and eigenenergies coalesce [28, 29]. So far, many interesting properties and promising applications have been found for \mathcal{PT} -symmetric systems, such as Bloch oscillations [30, 31], nonreciprocal and unidirectional invisible light propagations [14, 32, 33], coherent perfect absorbers [34–37], giant light amplification [38], single-mode lasers [39, 40], phonon lasers [41, 42], topological energy transfer [43], mode switching [44], enhanced sensing [40, 45], asymmetric diffraction [46, 47], quantum information [48, 49], and quantum state tomography [50], etc.

Recently, a class of multidimensional potentials invariant under complex conjugation and reflection in only one direction [e.g. $V^*(x, y) = V(-x, y)$ or $V^*(x, y) = V(x, -y)$ in two dimensions (2D)], called as *partial* \mathcal{PT} ($\text{p}\mathcal{PT}$) symmetric potentials, have been found theoretically to support all-real spectra. Interestingly, systems with such potentials display also phase transitions from the unbroken phase to the broken one [51, 52]. The study of the $\text{p}\mathcal{PT}$ symmetry can provide a way for realizing multidimensional potentials with all-real spectra without requiring strict \mathcal{PT} symmetry in high dimensions.

In this Letter, we report the first experimental observation of $\text{p}\mathcal{PT}$ symmetry and its phase transition. We consider a cesium atomic vapor driven by a probe and a control laser beams, both are half overlapped by a repumping laser beam, resulting in gain and loss for the

probe beam and hence the production of a 2D $p\mathcal{PT}$ -symmetric potential for the propagation of the probe beam. Furthermore, a transition of the $p\mathcal{PT}$ symmetry from an unbroken phase to a broken one is observed through adjusting the beam-waist ratio of the control and probe beams; the domains of unbroken, broken, and non- $p\mathcal{PT}$ phases are also discriminated clearly. In addition, a technique for precisely determining the location of the EP of the $p\mathcal{PT}$ symmetry breaking is developed through the measurement of the asymmetry degree of the probe intensity distribution. The theoretical analysis and numerical simulation based on Maxwell-Bloch equations are also carried out, which reproduce the all experimental observations well. The results on the $p\mathcal{PT}$ symmetry and its phase transition reported here open a route for actively manipulating multidimensional laser beams in non-Hermitian systems, and have potential applications for designing new light amplifiers and attenuators.

Experimental setup.— The schematic of the experimental setup and the related atomic excitation scheme is shown in Fig. 1. The experiment is performed with a room temperature cesium vapor cell of length 2 cm and diameter 2.5 cm. A weak probe and a strong control beams (with half Rabi frequencies Ω_p and Ω_c [53], respectively) are overlapped and co-propagate through the cell; see Fig. 1(b). They drive the atomic transitions $|1\rangle \rightarrow |3\rangle$ and $|2\rangle \rightarrow |3\rangle$, respectively, with detunings given by $\Delta_3 = \omega_p - (E_3 - E_1)/\hbar$ and $\Delta_2 = \omega_p + \omega_c - (E_2 - E_1)/\hbar$, where E_α is the eigenenergy of the atomic level $|\alpha\rangle$ ($\alpha = 1, 2, 3$) [see Fig. 1(a)].

Both the probe and the control beams are of Gaussian profiles and their $1/e^2$ waists are w_p and w_c , respectively. The beam-waist ratio of the control and probe beams is $\sigma \equiv w_c/w_p$, which is varied between 1.5 and 5 by tuning the waist of the control beam while keeping $w_p = 110 \mu\text{m}$. The repumping laser (half Rabi frequency Ω_r) has an elliptical Gaussian profile with $1/e^2$ waist $w_{r1} = 200 \mu\text{m}$ ($w_{r2} = 700 \mu\text{m}$) for short (long) axis. It counter-propagates through the cell and covers the half of probe and control beams [see the inset of Fig. 1(b)]. In this way, a 2D optical potential with the $p\mathcal{PT}$ symmetry [i.e. $V^*(x, y) = V(-x, y)$] for the probe propagation can form. After passing through the vapor cell, the probe beam is detected by a photodiode (PD) for monitoring its absorption and detected by a charge coupled device (CCD) for attaining its intensity distribution. The atomic density \mathcal{N}_a can be changed by varying the temperature of the cell placed in a thermal chamber (for more details, see the supplemental material [54]).

Observation of the $p\mathcal{PT}$ symmetry and its phase transition.— In the experiment, we lock the frequencies of the three laser beams such that $\Delta_2 = 0$ and $\Delta_3 = 2\pi \times 607 \text{ MHz}$, and the frequency of the repumping laser is resonant with $|1\rangle \rightarrow |3\rangle$. In the absence of the repumping beam, the probe beam experiences a loss (i.e. an absorption), which gives a PD signal S_L ; in the

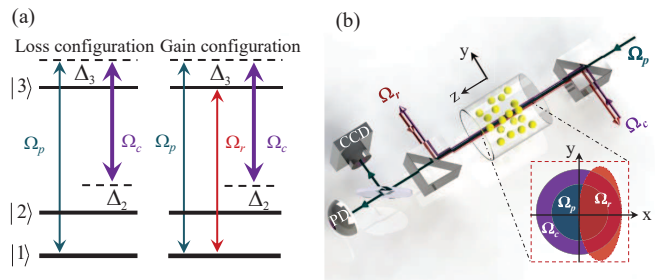


FIG. 1. Experimental design for observing the $p\mathcal{PT}$ symmetry and its phase transition. (a) Three-level excitation scheme of cesium atoms. A weak probe laser (Ω_p) couples the transition $|1\rangle \rightarrow |3\rangle$ and a strong control laser (Ω_c) couples $|2\rangle \rightarrow |3\rangle$, forming the loss configuration in the left panel, with Δ_j ($j = 2, 3$) frequency detunings. A repumping laser (Ω_r) resonantly drives the transition $|1\rangle \rightarrow |3\rangle$, forming the gain configuration in the right panel. (b) Sketch of the experimental setup. The control beam is fully overlapped with the probe beam, both of them are Gaussian and co-propagate through the cell. The repumping beam (with an elliptical Gaussian profile) counter-propagates with the probe and control beams and covers the right-half region of the probe beam (see the inset), which creates a 2D $p\mathcal{PT}$ -symmetric potential for the probe beam. The output probe beam is detected with PD and CCD camera.

presence of the repumping beam it experiences respectively a gain and a loss in the right- and left-half regions, which gives a PD signal S_{GL} . When the gain and loss are exactly balanced, the PD signal S_{GL} would be zero.

Shown in the upper part of Fig. 2(a) is the measured result of the probe intensity distribution from the CCD in the presence of the repumping beam for $\sigma = 2.14$. The intensity distribution is uniform (un-uniform) when $T < 29^\circ\text{C}$ ($T \gtrsim 29^\circ\text{C}$). The degree of asymmetry of the distribution for $T \gtrsim 29^\circ\text{C}$ is increased as T increases, which becomes the most evident at $T = 45^\circ\text{C}$, i.e. the intensity displays clearly half-dark (left) and half-bright (right) distribution. The orange circles shown in Fig. 2(a1) are results of the probe absorption (i.e. signal S_{GL}) measured from the PD as a function of T (\mathcal{N}_a). We see that S_{GL} keeps nearly zero for $T < 29^\circ\text{C}$ (or $\mathcal{N}_a < 6.29 \times 10^{10} \text{ cm}^{-3}$), indicating that the gain and loss are balanced and hence the system works in a regime of $p\mathcal{PT}$ symmetry (marked by the shadow square domain in the figure); S_{GL} begins to increase for $T \gtrsim 29^\circ\text{C}$, indicating that the gain-loss balance is lost and thus un-uniform intensity distribution occurs [corresponding to the lower row of Fig. 2(a)]. Note that this is not due to the breaking of the $p\mathcal{PT}$ symmetry (i.e. not phase transition), but due to the non- $p\mathcal{PT}$ symmetry resulted from the growth of the spontaneous emission of $|3\rangle$ as temperature increases. For comparison, the probe absorption in the absence of the repumping beam (i.e. signal S_L from PD) is also given by the blue squares in Fig. 2(a1), which increases with T (\mathcal{N}_a), indicating that the probe

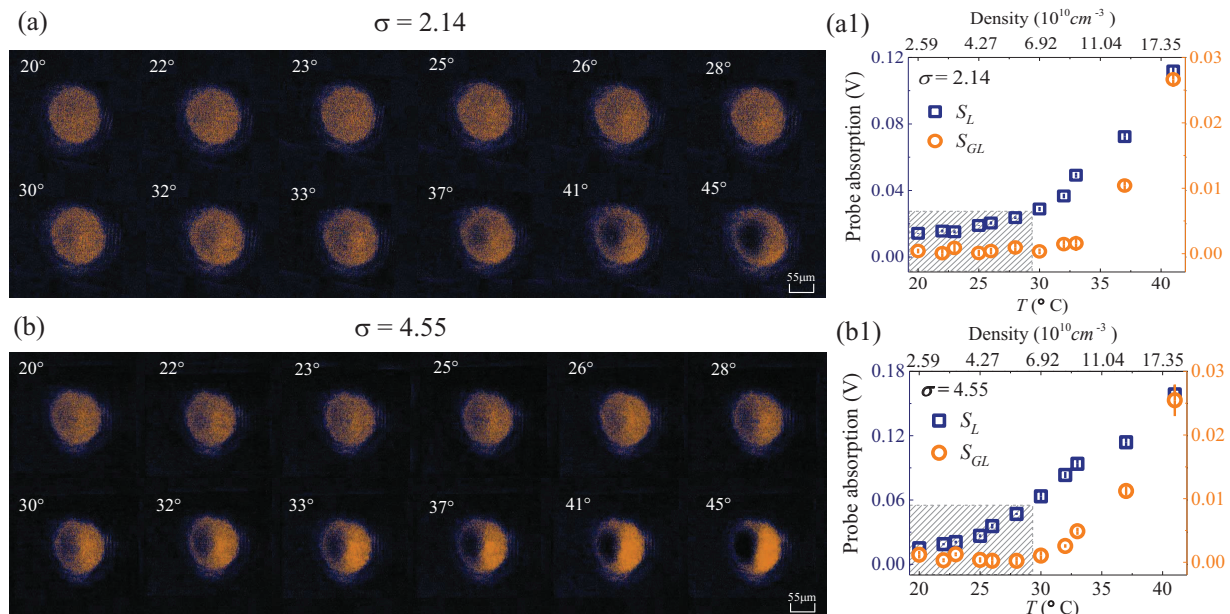


FIG. 2. Measurements of the $p\mathcal{PT}$ symmetry and its phase transition obtained by changing the atomic-cell temperature and the beam-waist ratio $\sigma \equiv w_c/w_p$ between the control and probe beams. (a) The measured result of the probe intensity distribution for $\sigma = 2.14$. The uniform (un-uniform) distribution observed for $T < 29^\circ\text{C}$ ($\gtrsim 29^\circ\text{C}$) indicates that the system works in a regime of the $p\mathcal{PT}$ symmetry (non- $p\mathcal{PT}$ symmetry). No $p\mathcal{PT}$ phase transition occurs in this case. (a1) Measured result of the probe absorption as a function of temperature T (atomic density N_a) with (orange circles) and without (blue squares) the repumping beam. S_{GL} (S_L): the PD signal in the presence (absence) of the repumping beam. Shadow square: the domain where the system works with the $p\mathcal{PT}$ symmetry. (b) and (b1) display similar measurements to (a) and (a1) but for $\sigma = 4.55$; in this situation, the probe beam displays an un-uniform intensity distribution for all temperatures due to the $p\mathcal{PT}$ symmetry and its phase transition into a broken $p\mathcal{PT}$ symmetry (see the text for details).

beam always suffers a significant loss and hence no $p\mathcal{PT}$ symmetry occurs.

In order to observe not only the $p\mathcal{PT}$ symmetry but also its phase transition in the system, we take σ as a tunable parameter and make new measurements. Plotted in Fig. 2(b) and (b1) are measured results similar to Fig. 2(a) and (a1) but for $\sigma = 4.55$. We see that in this situation the probe beam displays asymmetric intensity distributions for all temperatures [Fig. 2(b)]. Meanwhile, $S_{GL} \approx 0$ for $T < 29^\circ\text{C}$, meaning that the gain-loss balance is kept and the system works in a $p\mathcal{PT}$ -symmetric phase [the first row in Fig. 2(b) and the shadow domain in Fig. 2(b1)]. Consequently, the non-uniformity of the probe intensity distribution for $T < 29^\circ\text{C}$ [the first row of Fig. 2(b)] *must* be the outcome by $p\mathcal{PT}$ -symmetry breaking, i.e. the system has entered into a broken $p\mathcal{PT}$ -symmetric phase from the unbroken $p\mathcal{PT}$ -symmetric phase.

The above experimental findings can be analyzed quantitatively by defining the asymmetry degree of the probe intensity distribution

$$D_{\text{asym}} = (I_{p, \text{right}} - I_{p, \text{left}})/(I_{p, \text{right}} + I_{p, \text{left}}), \quad (1)$$

where $I_{p, \text{left}}$ ($I_{p, \text{right}}$) is the average of the probe intensity in the left-half (right-half) part of the distribution, with

$D_{\text{asym}} = 0$ and $D_{\text{asym}} \in (0, 1]$ characterizing uniform and un-uniform intensity distributions, respectively.

Measured (samples) and fitted (lines) results of D_{asym} as a function of T for $\sigma = 1.70, 2.14, 3.63, 3.95$ and 4.55 are shown in Fig. 3(a), respectively. We see that D_{asym} increases slowly with T ; however, it increases abruptly from 0 when σ exceeds a critical value σ_{cr} . Illustrated in Fig. 3(b) are measured (samples) and calculated (lines) results of D_{asym} as a function of σ , respectively for $T = 24^\circ\text{C}, 26^\circ\text{C}$, and 28°C . It reveals clearly that a phase transition of $p\mathcal{PT}$ symmetry indeed occurs, with the EP locating at $\sigma = \sigma_{cr} \simeq 3.8$. Based on Fig. 3(a) and (b), a phase diagram is obtained by taking D_{asym} as a function of T and σ in Fig. 3(c), where domains of the unbroken, broken, and non- $p\mathcal{PT}$ phases are displayed unambiguously. The solid (dashed) line indicates the boundary between domains of the unbroken $p\mathcal{PT}$ -symmetric phase and the broken one.

Theoretical analysis and numerical simulation.— The Maxwell-Bloch equations describing the probe propagation are solved by using a perturbation method for $\Omega_p \ll \Omega_c, \Omega_r$. Gain-loss property of the probe beam can be obtained from the linear dispersion relation of the system (see [54] for more details).

According to the experiment, the control-beam inten-

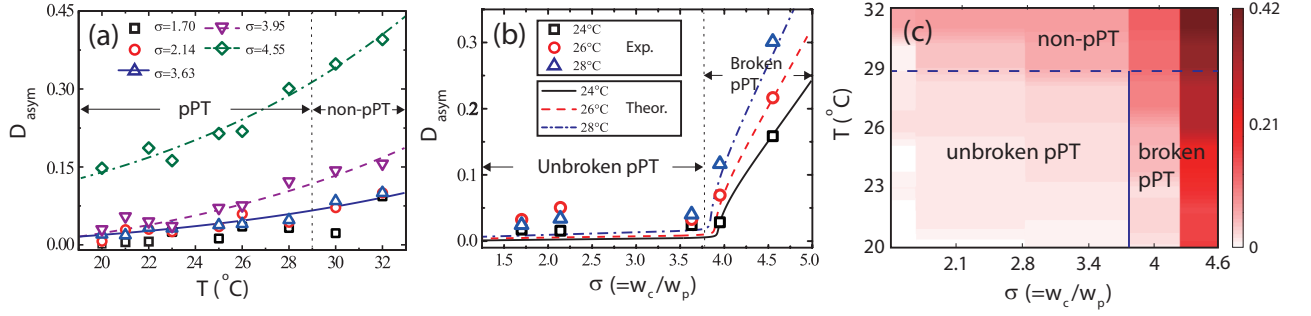


FIG. 3. Discrimination of the unbroken, broken, and non- $p\mathcal{PT}$ phases. (a) Measurements (samples) and fittings (lines) of the asymmetry degree D_{asym} as a function of temperature T for beam-waist ratio $\sigma = 1.70, 2.14, 3.63, 3.95$ and 4.55 , respectively. (b) Measurements (samples) and calculations (lines) of D_{asym} as a function of σ , respectively for $T = 24^\circ\text{C}, 26^\circ\text{C}$, and 28°C , with the EP locating at $\sigma = \sigma_{cr} \simeq 3.8$. (c) Phase diagram by taking D_{asym} as a function of T and σ , where domains of the unbroken, broken, and non- $p\mathcal{PT}$ phases are shown. The solid (dashed) line indicates the boundary between domains of the unbroken $p\mathcal{PT}$ -symmetric phase and the broken one.

sity has the form $I_c(\xi, \eta) \approx I_{c0}[1 - (\xi^2 + \eta^2)/\sigma^2]$, with $(\xi, \eta) = (x, y)/w_p$ and I_{c0} the maximum intensity [53]. The propagation equation of the probe beam takes the form $i\partial_\zeta \Omega_p = -d(\partial_\xi \xi + \partial_\eta \eta)\Omega_p - V(\xi, \eta)\Omega_p$, with $\zeta = z/L$; L is the cell length, $d = L/L_{\text{diff}}$ with $L_{\text{diff}} = 2k_p w_p^2$ the characteristic diffraction length. The potential in the equation, $V(\xi, \eta)$, can be written in the form $V(\xi, \eta) = V_1(\xi) + V_2(\eta)$. Here $V_1(\xi) = L(\beta_G \xi^2 + i\gamma_G)$ and $V_2(\eta) = L\beta_L \eta^2$ [$V_1(\xi) = L(\beta_L \xi^2 + i\gamma_L)$ and $V_2(\eta) = L\beta_L \eta^2$] for $\xi > 0$ ($\xi < 0$), where $\beta_{G,L} = \sigma^2 I_{c0} \text{Re}(\partial k_{G,L}/\partial I_c)|_{I_c=I_{c0}}$ and $\gamma_{G,L} = \text{Im}(k_{G,L} - \omega/c)|_{I_c=I_{c0}}$, with k_G (k_L) the linear dispersion relation with (without) the repumping laser. Thus, once the condition

$$\beta_G = \beta_L = \beta, \quad \gamma_G = -\gamma_L = \gamma, \quad (2)$$

is fulfilled, one has $V(\xi, \eta) = V^*(-\xi, \eta)$, i.e. $V(\xi, \eta)$ is $p\mathcal{PT}$ -symmetric potential.

From the above analysis we have the following conclusions (which are in agreement with the experimental results given above): (i) The location of EP of the $p\mathcal{PT}$ symmetry is determined by the ratio between the loss and gain, i.e. γ/β , which is not dependent on the atomic density \mathcal{N}_a . Thus, it is not available to observe the breaking of the $p\mathcal{PT}$ symmetry through increasing the atomic density (the cell temperature). (ii) The ratio γ/β is proportional to σ^2 . Therefore, one can observe the breaking of the $p\mathcal{PT}$ symmetry by increasing σ in the system.

For a further comparison between theory and experiment, the upper part of Fig. 4 shows the probe intensity distribution for $(\sigma, T) = (2.14, 28^\circ\text{C}), (4.55, 20^\circ\text{C}), (4.55, 24^\circ\text{C})$, and $(4.55, 30^\circ\text{C})$, respectively. The first (second) row is the result given by experiment (theory). The distribution is uniform in (a) and (a1) due to the perfect $p\mathcal{PT}$ symmetry, un-uniform in (b), (b1) and (c), (c1) due to the breaking of the $p\mathcal{PT}$ symmetry, and un-uniform in (d) and (d1) due to the non- $p\mathcal{PT}$ symmetry. We see that the theory agrees with the experiment well.

Applications for light amplifier and attenuator.— The

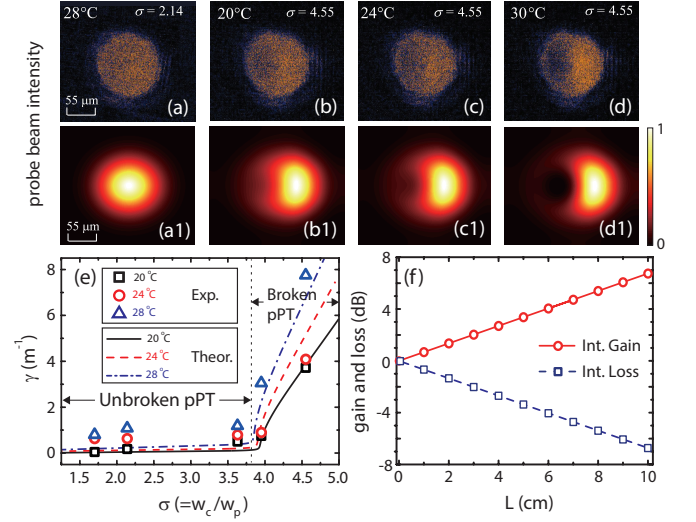


FIG. 4. The control of the $p\mathcal{PT}$ symmetry. (a)-(d) Measured result [for different (σ, T)] of the probe intensity distribution, which is uniform in (a) due to the unbroken $p\mathcal{PT}$ symmetry, un-uniform in (b) and (c) due to the broken $p\mathcal{PT}$ symmetry, and un-uniform in (d) due to the non- $p\mathcal{PT}$ symmetry. (a1)-(d1) Numerical results corresponding to (a)-(d). (e) Measured (samples) and calculated (lines) results of the gain and loss coefficient γ as a function of σ for different T . (f) Red circles (blue squares): the gain and loss of output probe intensity observed in the left (right) part of the probe beam as a function of the cell length L for $(\sigma, T) = (4.55, 28^\circ\text{C})$. The gain (loss) of the probe beam in the right (left) part can arrive 7 dB (-7 dB) at $L = 10$ cm.

relation between the gain-loss coefficient γ and the asymmetry degree of the probe intensity D_{asym} is given by

$$\gamma = \ln[(1 + D_{\text{asym}})/(1 - D_{\text{asym}})]/(4L). \quad (3)$$

Since the measurement of D_{asym} can reach a high precision (the relative standard deviation $\lesssim 5\%$), we can determine the location of EP rather precisely. Fig. 4(e) shows

a measurement (samples) and a simulation (lines) on γ as a function of σ for $T = 20^\circ\text{C}$, 24°C , and 28°C , respectively. Similar to Fig. 3(b), the mutation of γ clearly reveals the breaking of $p\mathcal{PT}$ symmetry with the location of EP ($\sigma_{cr} \simeq 3.8$). Fig. 4(f) shows the output probe intensities respectively in the right (gain) and left (loss) parts as functions of L ; one sees that for a 10-cm-long cell with $(\sigma, T) = (4.55, 28^\circ\text{C})$, the increase (decrease) of the probe intensity in the right (left) part can arrive 7 dB (-7 dB). Therefore, the present system is promising for designing new types of optical devices that can realize a light amplifier and attenuator in different parts of a single laser beam.

Conclusion.— We have carried out, for the first time, the experimental observation on $p\mathcal{PT}$ symmetry by using a laser-driven cesium atomic gas; the transition of the $p\mathcal{PT}$ symmetry from an unbroken phase to a broken one has been measured; the unbroken, broken, and non- $p\mathcal{PT}$ phases are discriminated clearly. We have also developed a technique to precisely determine the location of the EP of the $p\mathcal{PT}$ symmetry breaking. The experimental results have been verified well by theoretical calculations. Our work paves the way for controlling multidimensional laser beams in non-Hermitian optical systems, and have potential applications for designing new types of light amplifiers and attenuators.

J. Z. is supported by the National Key R&D Program of China (Grant No. 2017YFA0304203), the National Natural Science Foundation of China (Grant Nos. 61835007, 11434007, 61775124, and 11804202), Changjiang Scholars and Innovative Research Team University of Ministry of Education of China (Grant No. IRT_17R70) and 1331KSC. G. H., C. H., and Z. B. are supported by the National Natural Science Foundation of China (Grant Nos. 11975098, 11974117, and 11904104). C. H. is also supported by the National Key R&D Program of China (Grant Nos. 2016YFA0302103 and 2017YFA0304201), and Shanghai Municipal Science and Technology Major Project (Grant No. 2019SHZDZX01).

* Y. X. and C. H. contributed equally to this work.

† Corresponding author. gxhuang@phy.ecnu.edu.cn

‡ Corresponding author. zhaojm@sxu.edu.cn

- [1] C. M. Bender and S. Boettcher, Real Spectra in Non-Hermitian Hamiltonians Having PT Symmetry, *Phys. Rev. Lett.* **80**, 5243 (1998).
- [2] C. M. Bender, Introduction to PT-symmetric quantum theory, *Contemp. Phys.* **46**, 277 (2005).
- [3] C. M. Bender, Making sense of non-Hermitian Hamiltonians, *Rep. Prog. Phys.* **70**, 947 (2007).
- [4] V. V. Konotop, J. Yang, and D. A. Zezyulin, Nonlinear waves in PT-symmetric systems, *Rev. Mod. Phys.* **88**, 035002 (2016).
- [5] R. El-Ganainy, K. G. Makris, M. Khajavikhan, Z. H. Musslimani, S. Rotter, and D. N. Christodoulides, Non-Hermitian physics and PT symmetry, *Nat. Phys.* **14**, 11 (2018).
- [6] Y. Ashida, Z. Gong, and M. Ueda, Non-Hermitian physics, *Adv. Phys.* **69**, 249 (2020).
- [7] R. El-Ganainy, K. G. Makris, D. N. Christodoulides, and Z. H. Musslimani, Theory of coupled optical PT-symmetric structures, *Opt. Lett.* **32**, 2632 (2007).
- [8] Z. H. Musslimani, K. G. Makris, R. El-Ganainy, and D. N. Christodoulides, Optical Solitons in PT Periodic Potentials, *Phys. Rev. Lett.* **100**, 030402 (2008).
- [9] K. G. Makris, R. El-Ganainy, D. N. Christodoulides, and Z. H. Musslimani, Beam Dynamics in PT Symmetric Optical Lattices, *Phys. Rev. Lett.* **100**, 103904 (2008).
- [10] L. Feng, R. El-Ganainy, and L. Ge, Non-Hermitian photonics based on parity-time symmetry, *Nat. Photon.* **11**, 752 (2017).
- [11] A. Guo, G. J. Salamo, D. Duchesne, R. Morandotti, M. Volatier-Ravat, V. Aimez, G. A. Siviloglou, and D. N. Christodoulides, Observation of PT-Symmetry Breaking in Complex Optical Potentials, *Phys. Rev. Lett.* **103**, 093902 (2009).
- [12] C. E. Rüter, K. G. Makris, R. El-Ganainy, D. N. Christodoulides, M. Segev, and D. Kip, Observation of parity-time symmetry in optics, *Nat. Phys.* **6**, 192 (2010).
- [13] A. Szameit, M. C. Rechtsman, O. Bahat-Treidel, and M. Segev, PT-symmetry in honeycomb photonic lattices, *Phys. Rev. A* **84**, 021806(R) (2011).
- [14] L. Feng, M. Ayache, J. Huang, Y.-L. Xu, M.-H. Lu, Y.-F. Chen, Y. Fainman, and A. Scherer, Nonreciprocal light propagation in a silicon photonic circuit, *Science* **333**, 729 (2011).
- [15] A. Regensburger, C. Bersch, M. Miri, G. Onishchukov, D. N. Christodoulides, U. Peschel, Parity-time synthetic photonic lattices, *Nature (London)* **488**, 167 (2012).
- [16] B. Peng, Ş. K. Özdemir, F. Lei, F. Monifi, M. Gianfreda, G. L. Long, S. Fan, F. Nori, C. M. Bender, and L. Yang, Parity-time-symmetric whispering-gallery microcavities, *Nat. Phys.* **10**, 394 (2014).
- [17] L. Chang, X. Jiang, S. Hua, C. Yang, J. Wen, L. Jiang, G. Li, G. Wang, and M. Xiao, Parity-time symmetry and variable optical isolation in active-passive-coupled microresonators, *Nat. Photon.* **8**, 524 (2014).
- [18] J. Wen, X. Jiang, L. Jiang, and M. Xiao, Parity-time symmetry in optical microcavity systems, *J. Phys. B: At. Mol. Opt. Phys.* **51**, 222001 (2018).
- [19] L. Ding, K. Shi, Q. Zhang, D. Shen, X. Zhang, and W. Zhang, Experimental Determination of PT-Symmetric Exceptional Points in a Single Trapped Ion, *Phys. Rev. Lett.* **126**, 083604 (2021).
- [20] C. Hang, G. Huang, and V. V. Konotop, PT symmetry with a system of three-level atoms, *Phys. Rev. Lett.* **110**, 083604 (2013).
- [21] J. Sheng, M.-A. Miri, D. N. Christodoulides, and M. Xiao, PT-symmetric optical potentials in a coherent atomic medium, *Phys. Rev. A* **88**, 041803(R) (2013).
- [22] P. Peng, W. Cao, C. Shen, W. Qu, J. Wen, L. Jiang, and Y. Xiao, Anti-parity-time symmetry with flying atoms, *Nat. Phys.* **12**, 1139 (2016).
- [23] Z. Zhang, Y. Zhang, J. Sheng, L. Yang, M.-A. Miri, D. N. Christodoulides, B. He, Y. Zhang, and M. Xiao, Observation of Parity-Time Symmetry in Optically Induced Atomic Lattices, *Phys. Rev. Lett.* **117**, 123601 (2016).

- [24] R. Wen, C-L. Zou, X. Zhu, P. Chen, Z. Y. Ou, J. F. Chen, and W. Zhang, Non-Hermitian Magnon-Photon Interference in an Atomic Ensemble, *Phys. Rev. Lett.* **122**, 253602 (2019).
- [25] Y. Jiang, Y. Mei, Y. Zuo, Y. Zhai, J. Li, J. Wen, and S. Du, Anti-Parity-Time Symmetric Optical Four-Wave Mixing in Cold Atoms, *Phys. Rev. Lett.* **123**, 193604 (2019).
- [26] C. Hang and G. Huang, Parity-time symmetry with coherent atomic gases, *Adv. Phys. X* **2**, 737 (2017).
- [27] Z. Zhang, D. Ma, J. Sheng, Y. Zhang, Y. Zhang, and M. Xiao, Non-Hermitian optics in atomic systems, *J. Phys. B: At. Mol. Opt. Phys.* **51**, 072001 (2018).
- [28] W. Heiss, The physics of exceptional points, *J. Phys. A* **45**, 444016 (2012).
- [29] M-A. Miri and A. Alù, Exceptional points in optics and photonics, *Science* **363**, eaar7709 (2019).
- [30] S. Longhi, Bloch Oscillations in Complex Crystals with PT Symmetry, *Phys. Rev. Lett.* **103** 123601 (2009).
- [31] M. Wimmer, M. A. Miri, D. Christodoulides, and U. Peschel, Observation of Bloch oscillations in complex PT-symmetric photonic lattices, *Sci. Rep.* **5** 17760 (2005).
- [32] H. Ramezani, T. Kottos, R. El-Ganainy, and D. N. Christodoulides, Unidirectional nonlinear PT-symmetric optical structures, *Phys. Rev. A* **82**, 043803 (2010).
- [33] Z. Lin, H. Ramezani, T. Eichelkraut, T. Kottos, H. Cao, and D. N. Christodoulides, Unidirectional Invisibility Induced by PT-Symmetric Periodic Structures, *Phys. Rev. Lett.* **106** 213901 (2011).
- [34] S. Longhi, PT-symmetric laser absorber, *Phys. Rev. A* **82**, 031801(R) (2010).
- [35] Y. D. Chong, L. Ge, and A. D. Stone, PT-Symmetry Breaking and Laser-Absorber Modes in Optical Scattering Systems, *Phys. Rev. Lett.* **106**, 093902 (2011).
- [36] Y. Sun, W. Tan, H. Li, J. Li, and H. Chen, Experimental Demonstration of a Coherent Perfect Absorber with PT Phase Transition, *Phys. Rev. Lett.* **112**, 143903 (2014).
- [37] C. Hang, G. Huang, and V. V. Konotop, Tunable spectral singularities: coherent perfect absorber and laser in an atomic medium, *New J. Phys.* **18**, 085003 (2016).
- [38] V. V. Konotop, V. S. Shchesnovich, and D. A. Zezyulin, Giant amplification of modes in parity-time symmetric waveguides, *Phys. Lett. A* **376**, 2750 (2012).
- [39] L. Feng, Z. J. Wong, R. Ma, Y. Wang, and X. Zhang, Single-mode laser by parity-time symmetry breaking, *Science* **346**, 972 (2014).
- [40] H. Hodaei, M-A. Miri, M. Heinrich, D. N. Christodoulides, and M. Khajavikhan, Parity-time-symmetric microring lasers, *Science* **346**, 975 (2014).
- [41] H. Jing, S. K. Özdemir, X.-Y. Lü, J. Zhang, L. Yang, and F. Nori, PT-Symmetric Phonon Laser, *Phys. Rev. Lett.* **113** 053604 (2014).
- [42] J. Zhang, B. Peng, Ş. K. Özdemir, K. Pichler, D. O. Krimer, G. Zhao, F. Nori, Y-X. Liu, S. Rotter, and L. Yang, A phonon laser operating at an exceptional point, *Nat. Photonics* **12** 479 (2018).
- [43] H. Xu, D. Mason, L. Jiang, and J. G. E. Harris, Topological energy transfer in an optomechanical system with exceptional points, *Nature* **537** 80 (2016).
- [44] J. Doppler, A. A. Mailybaev, J. Böhm, U. Kuhl, A. Girschik, F. Libisch, T. J. Milburn, P. Rabl, N. Moiseyev, and S. Rotter, Dynamically encircling an exceptional point for asymmetric mode switching, *Nature* **537**, 76 (2016).
- [45] W. Chen, Ş. K. Özdemir, G. Zhao, J. Wiersig, and L. Yang, Exceptional points enhance sensing in an optical microcavity, *Nature* **548**, 192 (2017).
- [46] Y.-M. Liu, F. Gao, C.-H. Fan, and J.-H. Wu, Asymmetric light diffraction of an atomic grating with PT symmetry, *Opt. Lett.* **42**, 4283 (2017).
- [47] T. Shui, W.-X. Yang, S. Liu, L. Li, and Z. Zhu, Asymmetric diffraction by atomic gratings with optical PT symmetry in the Raman-Nath regime, *Phys. Rev. A* **97**, 033819 (2018).
- [48] L. Xiao, X. Zhan, Z. H. Bian, K. K. Wang, X. Zhang, X. P. Wang, J. Li, K. Mochizuki, D. Kim, N. Kawakami, W. Yi, H. Obuse, B. C. Sanders, and P. Xue, Observation of topological edge states in parity-time-symmetric quantum walks, *Nat. Phys.* **13**, 1117 (2017).
- [49] L. Xiao, T. Deng, K. Wang, G. Zhu, Z. Wang, W. Yi, and P. Xue, Non-Hermitian bulk-boundary correspondence in quantum dynamics, *Nat. Phys.* **16**, 761 (2020).
- [50] M. Naghiloo, M. Abbasi, Y. N. Joglekar, and K. W. Murch, Quantum state tomography across the exceptional point in a single dissipative qubit, *Nat. Phys.* **15**, 1232 (2019).
- [51] J. Yang, Partially PT symmetric optical potentials with all-real spectra and soliton families in multidimensions, *Opt. Lett.* **39**, 1133 (2014).
- [52] Y. V. Kartashov, V. V. Konotop, and L. Torner, Topological States in Partially-PT-Symmetric Azimuthal Potentials, *Phys. Rev. Lett.* **115**, 193902 (2015).
- [53] To realize the optical potential with $p\mathcal{PT}$ symmetry, Ω_c is taken to (x, y) -dependent (see [54]).
- [54] For more details, see the Supplemental Material at <http://link.aps.org/supplemental/0000> about our experimental setup, data analysis, and theoretical approach, which includes Refs. [51, 52, 55].
- [55] D. A. Steck, Cesium D Line Data, available online at <http://steck.us/alkalidata> (revision revision 1.6, 14 October 2003).